



## FLOW STRUCTURE OF HIGH REYNOLDS NUMBER FLOW IN A DUAL-ELBOW PIPING SIMULATING COLD-LEGS OF JSFR

H. TAKAMURA<sup>1,c</sup>, S. EBARA<sup>1</sup>, T. KANEKO<sup>2</sup>, H. YAMANO<sup>2</sup>, H. HASHIZUME<sup>1</sup>

<sup>1</sup> Department of Quantum Science and Energy Engineering, Graduate School of Engineering,  
Tohoku University, 6-6-01-2, Aramaki-aza-aoba, Aoba-ku, Sendai, Miyagi, 980-8579, Japan

<sup>2</sup> Advanced Nuclear System Research and Development Directorate, Japan Atomic Energy Agency,  
4002, Narita-cho, Oarai, Ibaraki, 311-1393, Japan

<sup>c</sup>Corresponding author: Tel.: +81227957906, Fax: +81227957906, Email: htaka@karma.qse.tohoku.ac.jp

### KEYWORDS:

**Main subjects:** multi elbow piping, flow visualization

**Fluid:** high Reynolds number flow

**Visualization method(s):** two dimensional Particle Image Velocimetry

**Other keywords:** Proper Orthogonal Decomposition, vortex shedding

**ABSTRACT:** Flow visualization experiments with 2D-PIV in a dual elbow system simulating the cold-leg piping of the JSFR were performed varying Reynolds number from  $0.3 \times 10^6$  to  $1.0 \times 10^6$ . The tested piping has two short elbows which are three-dimensionally connected with a straight pipe. This study investigated three-dimensional flow structures in the dual elbow system. Regarding the time averaged flow velocity, separated region appearing in the first elbow's intrados was shifted downstream compared with a single elbow system and gravitates toward the second one. The secondary flow between the two elbows had asymmetry Dean Vortices and changed into a swirling flow which swirls in the whole of the pipe. These could be caused by pressure field in the cross-section where the secondary flow generated. In the dual elbow system, separation vortices were shed from the separated region like a single elbow one. These vortices flowed by the intrados of the second elbow and its lower stream. The post-critical regime of the dual elbow flow may appear when Reynolds number is larger than about  $0.5 \times 10^6$ , as with the single elbow system.

**1. INTRODUCTION:** Japan Sodium-cooled Fast Reactor (JSFR) was designed as a fast breeder reactor of the 1.5 GW class in electric power in its conceptual design study [1, 2]. In the cooling system design, the number of the primary cooling loop has been reduced to two and short-radius elbow piping has been used in the loops. The short-radius elbow has the small curvature radius, which is equivalent to the pipe's diameter. A large diameter pipe and high flow velocity are necessary for a large flow rate per loop in the two loop system. Therefore, Reynolds ( $Re$ ) number for the flowing Sodium in the piping becomes extremely high up to the order of  $10^7$ . Under these conditions, the flow structure becomes very complex turbulent flow and large pressure fluctuations can be caused by vortices shed from the flow separated region near the intrados area of an elbow [3, 4]. The intrados means an interior curve of an elbow. These pressure fluctuations can sometimes cause a vibration of the whole piping and it is called Flow-Induced Vibration (FIV). The potential of the significant FIV in the JSFR should be evaluated for the safety reason and it is necessary to understand the flow structure in the short elbow piping flow with very high  $Re$  number. Because of the extremely high  $Re$  number in the reactor condition, the evaluation can be done by extrapolating from experimental data of a relatively low  $Re$  number condition in the range of post-critical regime of the elbow flow [5]. In the post-critical regime, some typical characteristics of the flow, such as dimensionless flow velocities and the total pressure loss coefficient, have been shown not to depend so much on  $Re$  number. The flow fields in the post-critical regime should be investigated in order to evaluate the potential FIV in the JSFR. Furthermore, experimental results can become the reference data for numerical simulations [6 – 8]. Cold-leg pipings of the primary cooling loop, supplying a coolant Sodium to the reactor core have three 90-degree elbows connected three-dimensionally. In the pipings,  $Re$  number reaches  $23 \times 10^6$  with the pipe diameter of 930 mm and the mean flow velocity of 8.4 m/s. They are considered to have very complex, unsteady and three-dimensional flow structures. Therefore, flow experiments should be carried out with single, dual and triple elbow layouts respectively in order to accumulate experimental results and investigate the complex flow clearly. Various flow experiments of the short elbow piping were carried out in the past. Shiraishi et al. reported the frequency



characteristic of pressure fluctuations and dimensionless velocity profiles in the short elbow piping [3, 4]. In this study, it was revealed that the pressure fluctuations had a prominent frequency component corresponding to a Strouhal number of about 0.5 near the flow separated region in the intrados of the elbow, and dimensionless velocity profile and the total pressure loss coefficient of the short elbow did not change so much in a wide range of  $Re$  number from about  $0.4 \times 10^6$  to about  $8.0 \times 10^6$ . Ono et al. reported the influence of the elbow curvature on the flow structure under high  $Re$  number condition ( $Re \sim 0.5 \times 10^6$ ) [9]. This study showed that the flow in a short-radius elbow piping had larger separated region in the intrados than that in a long-radius one and became more complex. Takamura et al. reported the three-dimensional flow structure and the frequency characteristics of flow velocity fluctuations in a short elbow piping [10]. This study revealed that the circumferential flows which flowed alternately into the intrados region in the opposite direction to each other were dominant in the flow field of the short elbow piping. As mentioned above, much knowledge about the flow structure in the single short elbow piping has been acquired already in the previous studies. Ebara et al. reported the averaged flow velocity fields and a few examples of the secondary flow for the dual elbow piping simulating the cold-leg by means of two-dimensional Particle Image Velocimetry (2D-PIV) [11]. However, in their study, the three dimensional flow structures and characteristics of the velocity fluctuation containing the separation vortex shedding were not investigated. In order to clarify them, more detailed measurements are required. That is to say, results of more cross section containing the secondary flow should be acquired and analyzed by various methods.

In this study, flow experiments for the dual elbow piping simulating the cold-leg of the JSFR are carried out in the post-critical regime by means of 2D-PIV. By using 2D-PIV, the flow field in the whole of a visualized cross section is obtained. Moreover, the three-dimensional flow structure should be investigated by a combination of results in more than one cross section. The detailed data about the secondary flow and fluctuation characteristics of flow velocity are acquired, and turbulent kinetic energy profiles and flow structure by means of Proper Orthogonal Decomposition (POD) analysis are argued. In addition, three-dimensional flow structure in the piping, the behavior of the separated vortices shed from the intrados region of the first elbow, the multiple elbow effect to the flow field and the post-critical regime of a dual elbow piping are also discussed. The multiple elbow effect means the effect of second elbow to the flow field downstream of the first elbow. The effect is supposed to be remarkable due to the short length of  $0.57 D$  between the two elbows in the cold-legs, where  $D$  is the diameter of the pipe. Because the flow field of a single elbow piping is well investigated in the previous studies, the effect can be indicated by comparing the flow field obtained from this study to that of the previous ones. On the other hand, the post-critical regime of a dual elbow piping has yet to be clarified and needs to be investigated so as to extrapolate from experimental data obtained from relatively low  $Re$  number conditions to the JSFR condition. Furthermore, this knowledge can be connected with the post-critical regime of a triple elbow piping simulating the full cold-leg piping of JSFR. The post-critical regime in a short single elbow flow appears when  $Re$  number is larger than about  $0.4 \times 10^6$ . If the flow characteristics in the dual elbow obtained from this experiment do not depend on  $Re$  number in the range of this experiment, the existence of the post-critical regime of a dual elbow piping can be suggested.

**2. Experimental Loop and Method:** Figure 1 shows a schematic of the experimental loop employed in this study. The loop is composed of a pump controlled by an inverter, a mixing tank, a straightener and a test section. The piping with a diameter,  $D$ , of 126.6 mm is mainly made of stainless steel. Working fluid is tap water at 45 degrees Celsius. Arbitrary  $Re$  number in the range from  $0.3 \times 10^6$  to  $1.0 \times 10^6$  is available by adjusting the flow velocity (1.47 ~ 4.78 m/s). An entrance section of  $28 D$  in length is installed upstream of the test section to obtain the fully developed turbulent pipe flow as the inlet condition. Mean flow velocity is measured by an ultrasonic flowmeter at the entrance section. The test section with a water jacket is made of acrylic resin and has two 90-degree short-radius elbows with a straight part of  $0.57 D$  length between the two elbows. Two elbows are three-dimensionally connected as shown in Figure 2 and curvature ratio of the elbows is 1.0, which is simulating the cold-leg of the JSFR. For the PIV measurement, a CCD camera with 1024x1024 pixels is used together with a diode laser oscillation emitting pulsed laser sheets of about 2 mm thickness with 808~815 nm wavelength. Tracer particles are nylon particles of 20  $\mu\text{m}$  in diameter, and 1024 time-series data of velocity vectors is obtained per one measurement. Separation time of the double pulse laser is varied from 100 to 400  $\mu\text{s}$ . All time-averaged velocities and turbulent kinetic energy distributions are calculated from 1024 time-series data of one shot. In the experiment, two kinds of cross-sections are visualized mainly. One is a cross-section which contains a curvature radius of the elbow, referred as to “flow cross-section” in this paper, and the other is that perpendicular to the channel centerline, “pipe cross-section”.

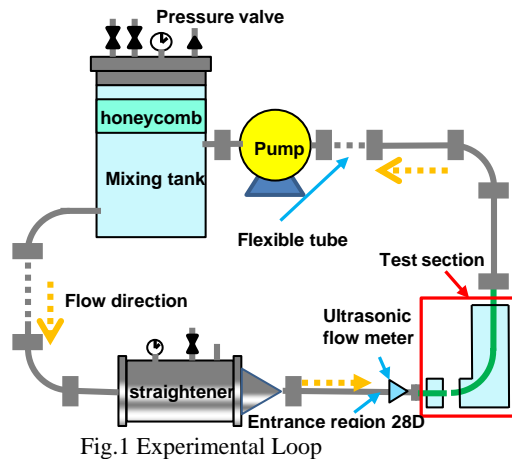


Fig.1 Experimental Loop



Fig.2 Cold-leg piping of the JSFR

**3. RESULT AND DISCUSSION:** The experiment was performed for Reynolds ( $Re$ ) number of between  $0.3 \times 10^6$  and  $1.0 \times 10^6$ . The flow fields in  $Re$  number of  $1.0 \times 10^6$  are mainly discussed as a representative and the  $Re$  number dependency of flow fields is mentioned later. At first, the flow fields when  $Re$  number is  $1.0 \times 10^6$  in the flow-cross section of the first elbow are shown. The position and the viewpoint of the cross section, the time averaged flow fields and the turbulent kinetic energy distribution normalized by the mean flow velocity are shown in Figure 3, 4 (a) and 4 (b), respectively. The separated region is formed in the intrados as shown in Fig. 4 (a) where the region is masked. In this paper, the flow separated region is defined as a region where the streamwise velocity regurgitates. The angle  $\theta$  stands for the angle between the first elbow's inlet and the starting point of the separated region in the visualized cross-section, and the  $x$  stands for the distance between the first elbow's outlet and the reattachment point in the visualized cross-section as shown in Fig. 4 (a). Fig. 4 (a) shows that the flow velocity is low in the separated region and its lower stream, and there is a large velocity gradient between these regions and the high velocity region in the center of a pipe. The flow fluctuates strongly along the shear flow region from the starting point of flow separation as shown in Fig. 4 (b). Moreover, the velocity fluctuation is also large in the downstream of the separated region. This characteristic is similar to that of a single elbow system, where the flow velocity fluctuates strongly in the lower stream of separated region due to the secondary flow acting as a transporter of large momentum in the high velocity region to the intrados [9, 10]. The similar flow field observed in the dual elbow system indicates that the flow structure is fundamentally the same between both elbow systems. In order to investigate the difference of flow fields between the single and dual elbow systems, in other words, the multiple elbow effect, the secondary flow between two elbows is scrutinized in the pipe cross-section. Figures 5 and 6 – 8 show the viewpoint of the cross-section and time-averaged velocity vector fields and non-dimensionalized turbulent kinetic energy distributions in each cross section, respectively. The positions of cross sections in Fig. 6 – 8 are at  $0 D$ ,  $0.4 D$  and  $0.57 D$  downstream from the first elbow's outlet, respectively. The position of  $0.57 D$  downstream of the first elbow's outlet corresponds to the the second elbow's inlet. Dean vortices which are typical of a curved pipe flow are observed as shown in Figs. 6 – 8. Moreover, there is a very low velocity region near the intrados of the first elbow as shown in Fig. 6 (a). It is considered the flow separated region because fluid does not flow into that region as shown in Fig. 6 (a). It is also found that the flow velocity fluctuates strongly in that region as shown in Fig. 6 (b). The secondary flow is almost symmetry at the first elbow's outlet as shown in Figs. 6 and gradually becomes asymmetry as it goes downstream as shown in Figs. 7 and 8. A pair of the circumferential flows is observed in the first elbow's intrados as shown in Fig. 6 (a), which takes the opposite direction to each other and reach about 65 % of the mean flow velocity 4.7 m/s. Moreover, one of them in the counter-clockwise direction becomes lower and the other in the clockwise direction becomes higher as it goes downstream as shown in Figs. 6 – 8. This can be inferred as follows. It is considered that the pressure increases in the extrados and decreases in the intrados in an curved pipe flow, and a similar pressure field can be formed in the dual elbow system. The circumferential flows in the counter-clockwise direction in Figs. 6 – 8 are decelerated because it flows from the intrados to the extrados and the circumferential flows in the clockwise direction are accelerated, vice versa. Therefore, compared with a single elbow system, the flow separated region is deformed to gravitate toward the intrados of the second elbow. High turbulent kinetic energy region is also shifted to the intrados of the second elbow as shown in Fig. 7 and 8. Figure 9 shows the starting point and the reattachment point expressed with  $\theta$  and  $x$ , respectively, varying with  $Re$  number. In order to find how the separated



region is shifted to the intrados of the second elbow, the flow cross-section is shifted parallel to the original one as shown in Figure 10. Fig. 9 (b) shows that  $x/D$  becomes large as the visualized cross-section gets away from the flow cross-section, and the reattachment point is shifted downstream. The maximum value of  $x/D$  can exist between 6 mm shift and 9 mm shift as shown in Fig. 9 (b) and let it be 7.5 mm tentatively. If the angle  $\varphi$  is defined as shown in Figure 11, the position of the reattachment points in the circumferential and axis directions are considered at about  $\varphi = 6.8$  degree and  $x/D = 0.35$ , respectively. In the secondary flow of a single elbow system, the velocity fluctuation is large in the downstream of the separated region in the intrados and the distribution is symmetry [10]. In the  $0.4 D$  downstream of the first elbow outlet, high turbulent kinetic energy region lies at about  $\varphi = 7$  degrees and just downstream of the reattachment point of the flow separation as shown in Fig 7 (b). This should be the supporting evidence of the shifted separated region. The reattachment point in the axis direction of the dual elbow system is shifted downstream compared with that of the single elbow system as shown in Fig. 9 (b). This can be considered because the velocity recovery by the circulating secondary flow decreases. Regarding the  $Re$  number dependency in the single and dual elbow system, Fig. 9 shows a tendency to be constant for  $Re$  number larger than about  $0.5 \times 10^6$ . In order to evaluate  $Re$  number dependency of the secondary flow, investigations are made for three secondary flows at  $0.2 D$  downstream of the outlet of the first elbow when  $Re$  number is  $0.3 \times 10^6$ ,  $0.5 \times 10^6$  and  $1.0 \times 10^6$ , respectively. Figures 12 show time-averaged velocity vector distributions of the three secondary flows normalized by each mean flow velocity. There cannot be seen a large difference among three flow fields. Moreover, flow fields in  $Re$  number of  $0.5 \times 10^6$  and  $1.0 \times 10^6$  have an almost identical velocity distribution. The above statements show that the flow field in the dual elbow piping has a difference from that in the single one. However, the lower limit of the post-critical regime in terms of  $Re$  number does not change a lot [3, 4, 10]. Therefore, the results of the experiment have the possibility to be extrapolated to the JSFR condition.

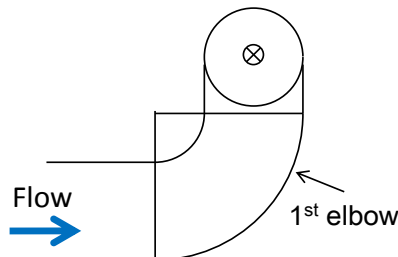


Fig.3 Viewpoint of the flow-cross section in the first elbow and its lower stream

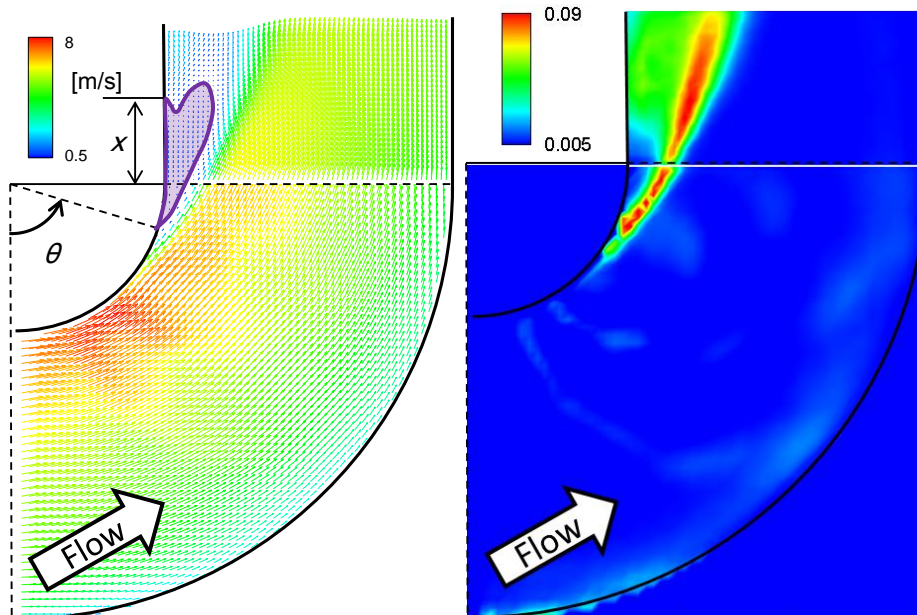


Fig.4 (a)

Fig.4 (b)

Fig.4 (a) Time averaged flow velocity vector field and (b) turbulent kinetic energy distribution of the flow-cross section in the first elbow and its lower stream at  $Re$  number of  $1.0 \times 10^6$

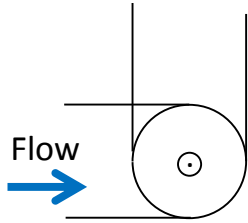


Fig.5 Viewpoint of the pipe-cross section between two elbows

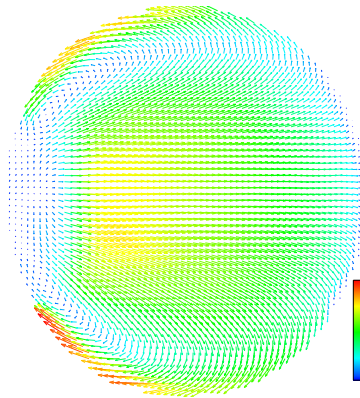


Fig.6 (a)

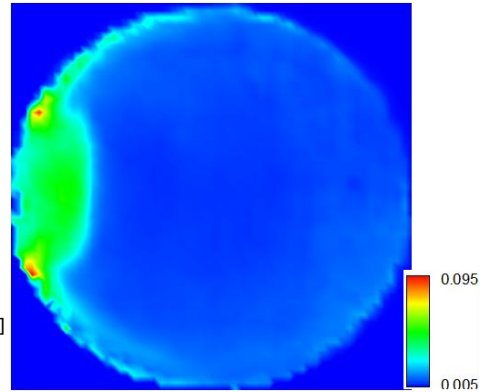


Fig.6 (b)

Fig.6 (a) Time averaged velocity field and (b) turbulent kinetic energy distribution in the first elbow's outlet at  $Re$  number of  $1.0 \times 10^6$

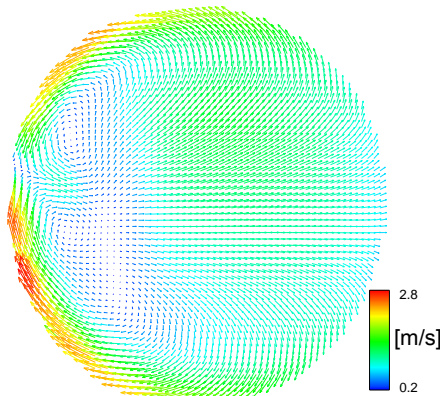


Fig.7 (a)

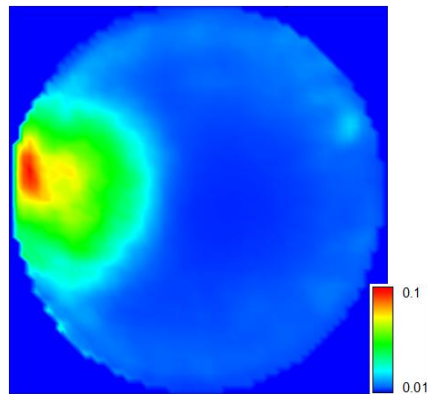


Fig.7 (b)

Fig.7 (a) Time averaged velocity field and (b) turbulent kinetic energy distribution in the  $0.4 D$  lower stream from the first elbow's outlet at  $Re$  number of  $1.0 \times 10^6$

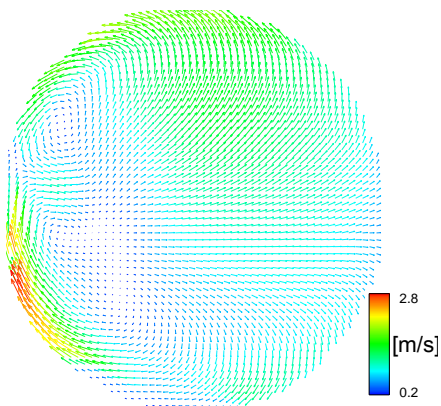


Fig.8 (a)

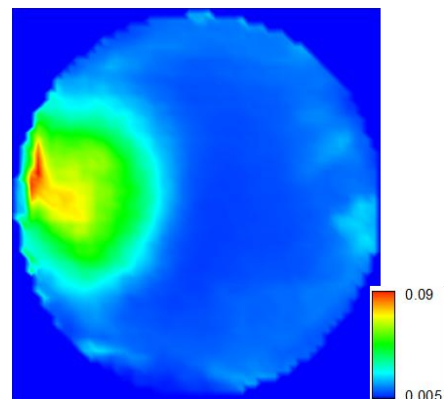


Fig.8 (b)

Fig.8 (a) Time averaged velocity field and (b) turbulent kinetic energy distribution in the  $0.57 D$  lower stream from the first elbow's outlet at  $Re$  number of  $1.0 \times 10^6$

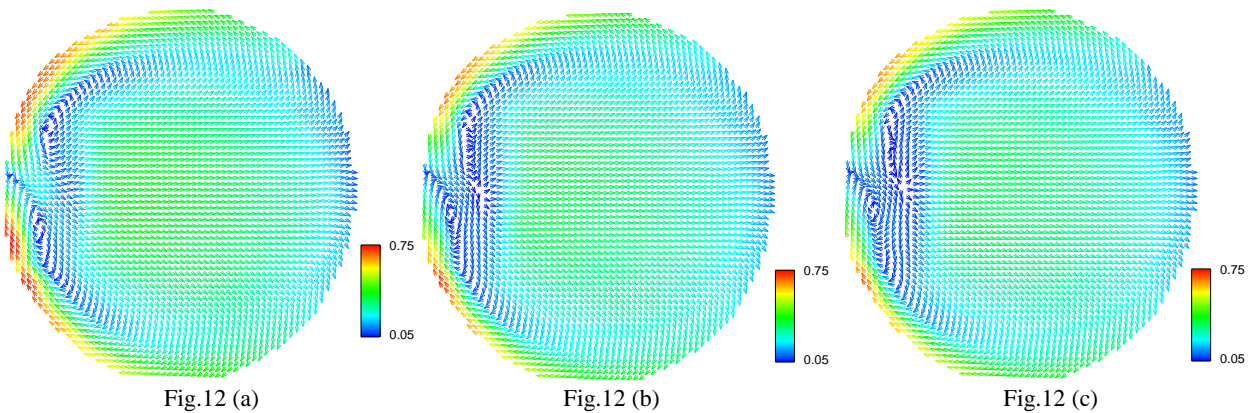
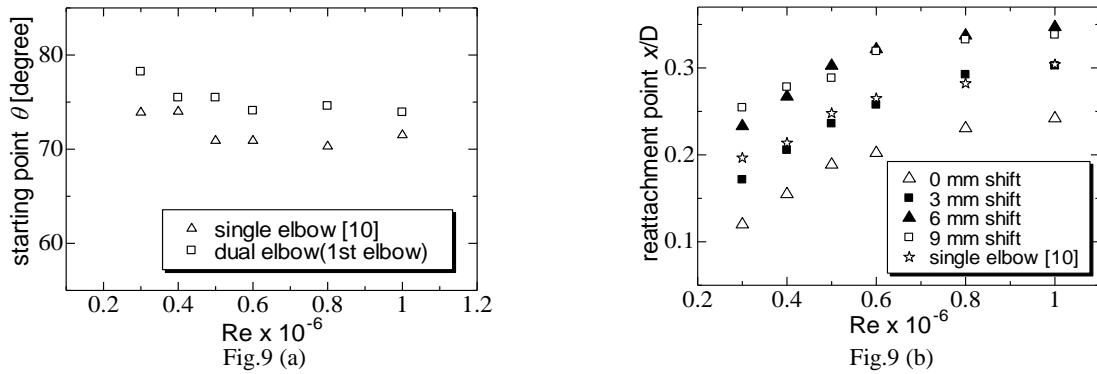
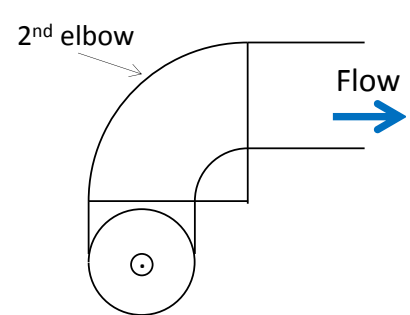
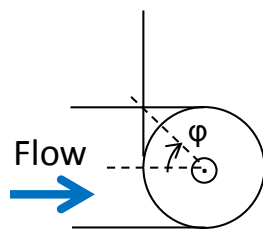
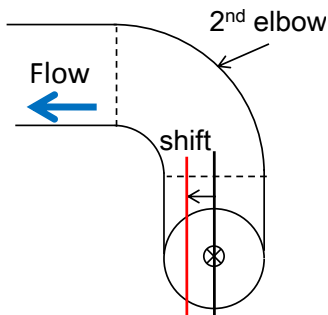


Fig.12 Time averaged flow fields in the pipe-cross section of the  $0.2 D$  lower stream of the first elbow's outlet.  $Re$  number of (a) is  $0.3 \times 10^6$ , (b) is  $0.5 \times 10^6$  and (c) is  $1.0 \times 10^6$ . These are normalized by the mean flow velocity.



Regarding results of the flow-cross sections in the second elbow and its downstream, the position and viewpoint, the time-averaged flow velocity field and the turbulent kinetic energy distribution are shown in Figures 13 and 14 respectively. Furthermore, the position and viewpoint of the secondary flow in the downstream of the second elbow and time-averaged flow velocity fields and turbulent kinetic energy distributions are shown in Figures 15 and 16 – 18, respectively. There can be seen a high velocity region near the intrados of the second elbow, and a flow separation does not appear like the first elbow as shown in Fig. 14 (a). This flow pattern shown in the second elbow can be attributed to pressure field formed in the pipe. Typically, it is considered that a high pressure region in the extrados of an elbow and a low pressure region in the intrados are formed in an elbow piping flow. Moreover, an adverse pressure gradient can cause a flow separation. However, when the circulating secondary flow exists, the fluid is exchanged between the high pressure region and the low pressure region, i.e., pressure recovery occurs in the intrados region.. In this case, the flow separation isn't easy to occur. Therefore, a flow separation does not appear in the second elbow. Besides this pressure field, a swirling flow formed in the second elbow, as mentioned below, is one of the reasons to prohibit flow separation from occurring because of its effect to press fluid onto the channel wall.

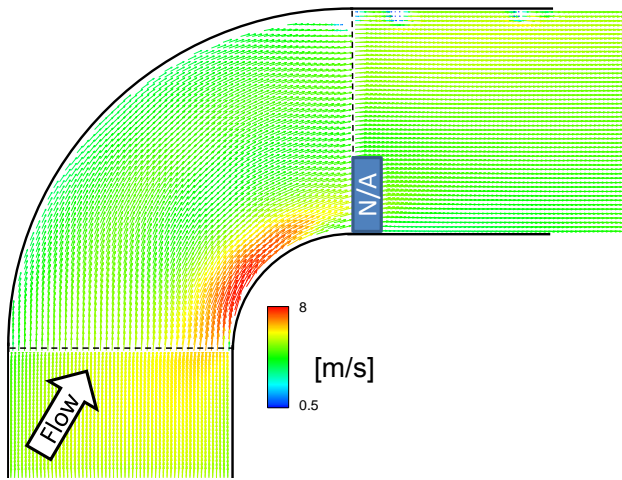


Fig.14 (a)

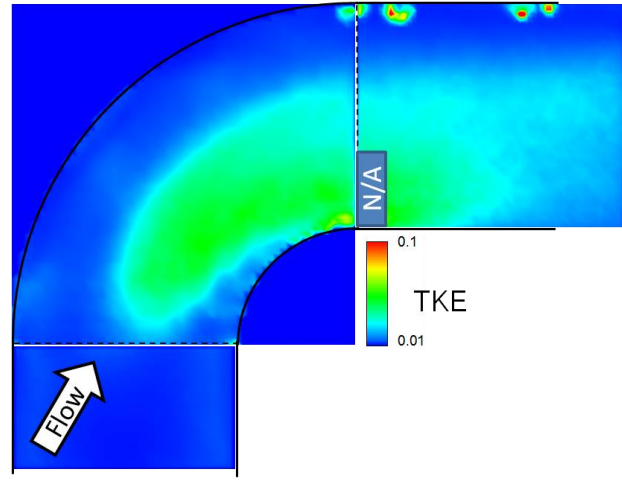


Fig.14 (b)

Fig.14 (a) Time averaged flow field and (b) turbulent kinetic energy distribution of the flow-cross section in the second elbow and its lower stream at  $Re$  number of  $1.0 \times 10^6$

Regarding the velocity fluctuation, strong fluctuating flow is not observed upstream of the inlet of the second elbow and the intrados as shown in Fig. 14 (b). Moreover, there is not any large production of velocity fluctuation in and downstream of the second elbow. With considering the above-statements, the strong fluctuating flow in Fig. 14 (b) should be transported from the first elbow. The swirling flow appears in the counter-clockwise direction from the figure's viewpoint and the circumferential flow in the clockwise direction only near the wall of the intrados as shown in Figs. 16 – 18. The center of swirling is eccentric and approaches the extrados of the second elbow. The especially strong swirling component is observed near the wall in the left side of Figs. 16 – 18 and reaches about 45 % of the mean flow velocity. It is lower than that of the circumferential flow between the elbows but exits in a wider region around the whole of the pipe-cross-section. This swirling flow can be considered to be attributed to the circumferential flow in the clockwise direction in Figs. 6 – 8 which is formed in the first elbow. It can be inferred that this flow grows into the swirling flow in the second elbow. The time-averaged secondary flow does not change a lot as it goes downstream as shown in Figs. 16 – 18 and the velocity field is almost uniform as shown in Fig. 14 (a). Therefore, the swirling flow should stably go downstream according to inertia. In the cold-les piping of the JSFR, there is the third elbow  $6.4 D$  downstream of the second elbow outlet and its inlet flow condition is suggested to be a swirling flow. Regarding the fluctuating component in the pipe cross-section, the turbulent kinetic energy is high mainly in the intrados of the second elbow, and the position where the highest turbulent kinetic energy appears shifts in the counter-clockwise direction as it goes downstream as shown in Figs. 16 – 18. This is because the velocity fluctuation is transported by the swirling flow.

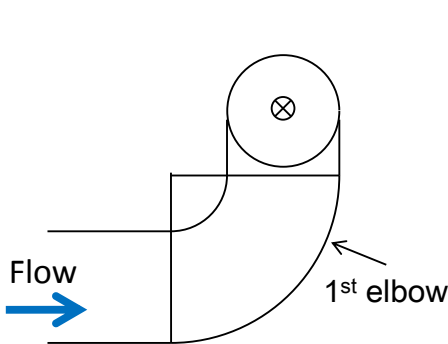


Fig.15 Viewpoint of the pipe-cross section in the second elbow

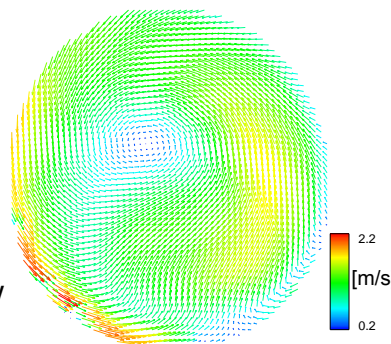


Fig.16 (a)

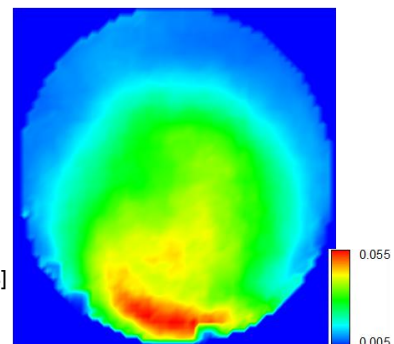


Fig.16 (b)

Fig.16 (a) Time averaged flow field and (b) turbulent kinetic energy distribution in the pipe-cross section of the second elbow's outlet at  $Re$  number of  $1.0 \times 10^6$

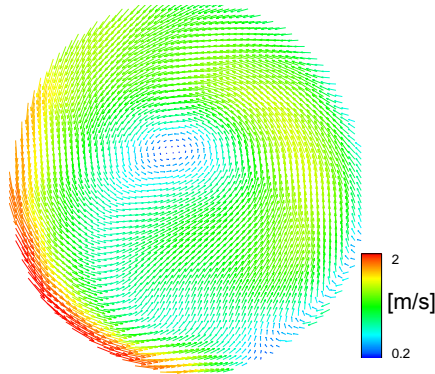


Fig. 17 (a)

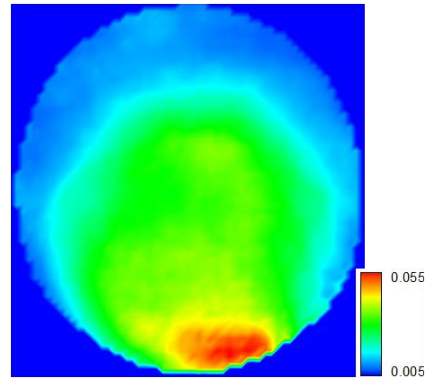


Fig.17 (b)

Fig.17 (a) Time averaged flow field and (b) turbulent kinetic energy distribution in the pipe-cross section of the 0.2  $D$  lower stream from the second elbow's outlet at  $Re$  number of  $1.0 \times 10^6$

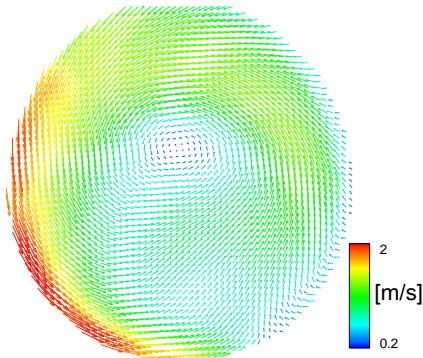


Fig.18 (a)

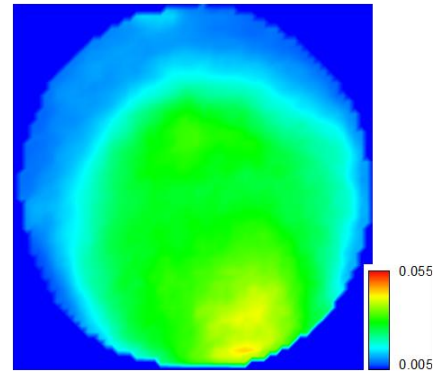


Fig.18 (b)

Fig.18 (a) Time averaged flow field and (b) turbulent kinetic energy distribution in the pipe-cross section of the 0.6  $D$  lower stream from the second elbow's outlet at  $Re$  number of  $1.0 \times 10^6$

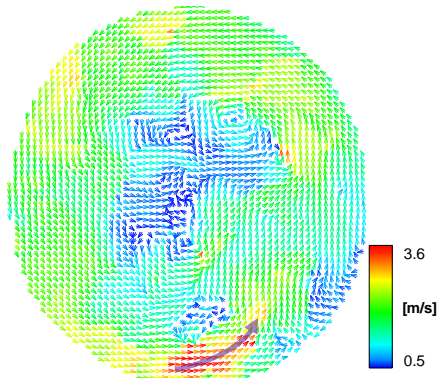


Fig.19 (a)

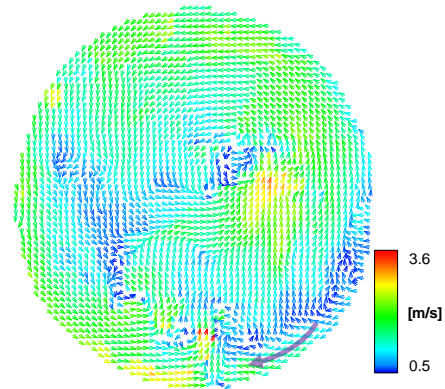


Fig.19 (b)

Fig.19 Two patterns of instantaneous flow fields in the pipe-cross section of the 0.2  $D$  lower stream from the second elbow's outlet at  $Re$  number of  $1.0 \times 10^6$

In order to see the detail of the flow velocity fluctuation, two patterns of instantaneous secondary flows in the 0.2  $D$  downstream of the second elbow are shown in Figures 19. The whole flow field swirls in the counter-clockwise direction and the especially strong circumferential flow is observed near the intrados as shown in Fig. 19 (a). Fig. 19 (b) shows a similar swirling flow but the circumferential flow in the clockwise direction also exists near the intrados. In the secondary flow between two elbows, the circumferential flows in clockwise and counter-clockwise directions flow toward the inside wall alternately with separation vortex shedding. In the lower stream of the second elbow, these circumferential flows seem to change into two patterns in Fig. 19 through the second elbow. Therefore, the separation vortex shed from the first elbow should flow near the intrados of the second elbow's outlet and its lower stream. Therefore, the vortex should periodically change the pressure near the intrados of the second elbow's outlet.



Proper Orthogonal Decomposition (POD) analysis is used in order to investigate fluctuating flow fields in the secondary flows more minutely and objectively [12]. POD analysis can analyze fluctuating flow fields and can extract coherent flow structures. Applying POD analysis to data of 2D-PIV is assumed to capture a structure of fluctuating flow fields which is not captured by observation of instantaneous flow fields. Figure 20 shows POD basis modes with contribution ratio in the secondary flow  $0.4 D$  downstream of the first elbow outlet and Figure 21 shows those  $0.2 D$  downstream of the second elbow's outlet. The mode whose contribution ratio is more than 5 % is selected as a primary basis mode in this paper and it is shown in the figures. The circumferential component is strong near the first elbow's intrados in the first and second POD mode as shown in Fig. 20. Moreover, in the third POD mode, the circumferential fluctuation occurs in the whole pipe region. The contribution ratio of the first mode is twice as high as that of the second mode and therefore, the circumferential velocity fluctuation near the intrados is considered as a dominant flow structure as shown in Fig. 20. This flow structure has a close relationship with the velocity recovery and the ejection of separation vortices in the single elbow piping flow [9, 10], almost the same flow structure occurs in the first elbow of the dual elbow system. Regarding the downstream of the second elbow, the flow field downstream of the second elbow fluctuates in a wider region than that downstream of the first elbow as shown in Fig. 21. Moreover, the first and second modes have a large vortex, respectively. These two vortices have different centers of rotation. The third mode has a very complex structure which has plural vortices. And therefore, the fluctuating flow field downstream of the second elbow is very complex and has multiple vortex structures. The contribution ratios of the first and second modes are close comparatively and that of the first mode is twice as high as that of the third mode. Therefore, the first and second modes are dominant flow structures in the flow fields. The two modes show that the circumferential fluctuation is strong near the intrados of the second elbow and the center of swirling also fluctuates. Moreover, the flow structure becomes very complex by the addition of the third POD mode.

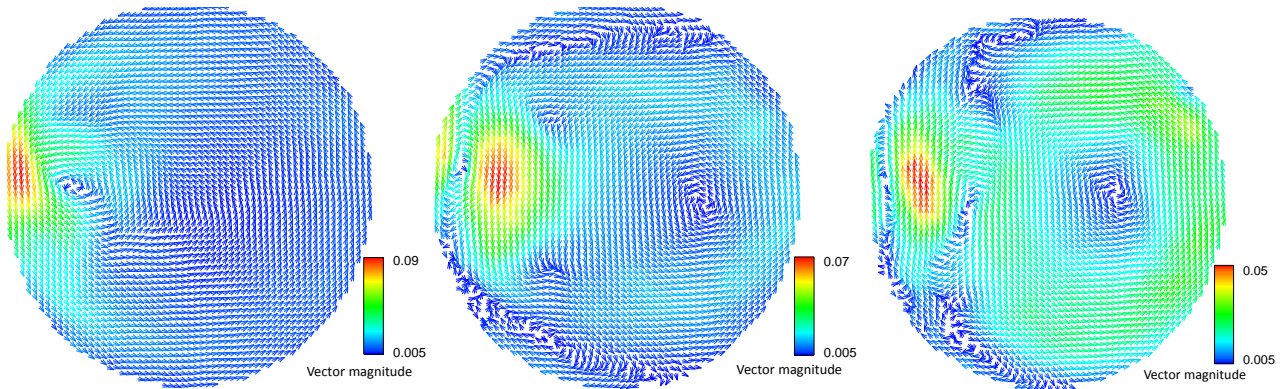


Fig.20 (a)-13.7%

Fig.20 (b)-6.28%

Fig.20 (c)-5.72%

Fig. 20 POD modes of the flow field in the  $0.4 D$  lower stream from the first elbow's outlet at  $Re$  number  $1.0 \times 10^6$ .

(a) the first mode, (b) the second mode and (c) the third mode. (with contribution ratio of each mode)

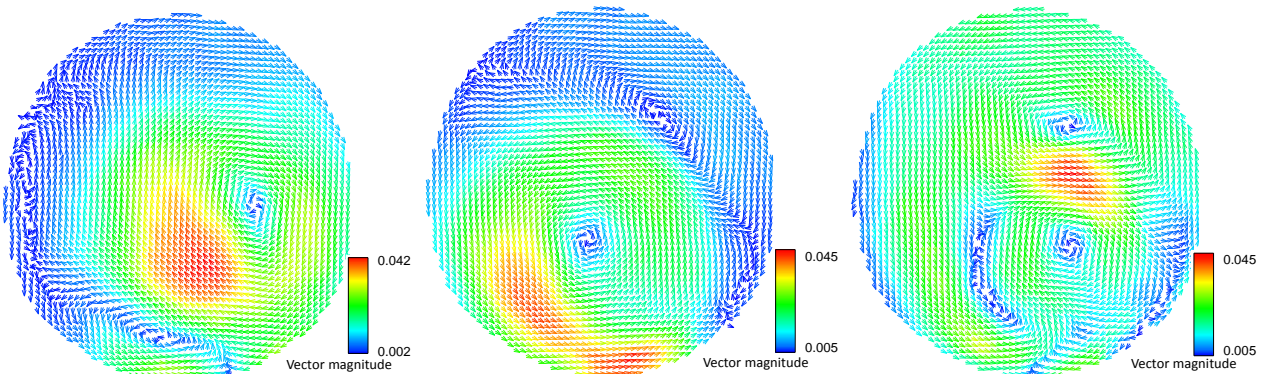


Fig.21 (a)-11.4%

Fig.21 (b)-9.06%

Fig.21 (c)-5.48%

Fig.21 POD modes of the flow field in the  $0.2 D$  lower stream from the second elbow's outlet at  $Re$  number  $1.0 \times 10^6$ .

(a) the first mode, (b) the second mode and (c) the third mode. (with contribution ratio of each mode)



#### 4. CONCLUSION

The flow visualization experiment with 2D-PIV in the dual elbow system simulating the cold-leg piping of the JSFR was performed. The findings are listed as follows.

- (1) The flow separation occurs in the first elbow and the reattachment points in the circumferential and axis directions are shifted to about  $\varphi = 7$  degrees and  $x/D = 0.35$ , respectively, when the  $Re$  number is  $1.0 \times 10^6$ . The separated region gravitates toward to the intrados of the second elbow and deforms compared with a single elbow system.
- (2) Dean vortices are formed in the secondary flow between two elbows as a similar manner of a single elbow system. Their fluctuating aspect has a close relationship with the velocity recovery and the ejection of the separation vortices. Moreover, their separation vortices should flow by the inside of the second elbow's outlet and periodically change the pressure.
- (3) Regarding the secondary flow downstream of the second elbow, the time-averaged flow field is a swirling flow. The fluctuating circumferential flows which are dominant flow structures between two elbows seem to change the fluctuating circumferential flows near the second elbow's intrados through the second elbow.
- (4) The flow structure in the dual elbow system is different from that in the single one. However, the lower limit of the post-critical regime in terms of  $Re$  number does not change a lot and the flow in the dual elbow system is regarded as the post-critical regime when  $Re$  number is larger than about  $0.5 \times 10^6$ .

#### References

1. Yamano, H. et al. *Unsteady Elbow Pipe Elbow to Develop a Flow-Induced Vibration Evaluation Methodology for Japan Sodium-Cooled Fast Reactor*. *Journal of Nuclear Science and Technology*. 2011. Vol. 48, No. 4, pp. 677-687
2. Aoto, K. et al. *Design study and R&D progress on Japan sodium-cooled fast reactor*. *Journal of Nuclear Science and Technology*. 2011. Vol. 48, issue 4, pp. 463-471
3. Shiraishi, T. et al. *Resistance and Fluctuating Pressures of a Large Elbow in High Reynolds Numbers*. *Journal of Fluids Engineering*. 2006. Vol. 128, pp. 1063-1073
4. Shiraishi, T. et al. *Pressure Fluctuation Characteristics of the Short-Radius Elbow Pipe for FBR in the Postcritical Reynolds Regime*. *Journal of Fluid Science and Technology*. 2009. vol. 4, No. 2, pp. 430-441
5. Idelchik, I. E., "Handbook of Hydraulic Resistance." Second Edition, Hemisphere Publishing Co., (1986)
6. Aizawa, K., et al. *Numerical calculation of fluid flow within a large-diameter piping with a short-radius elbow in JSFR*. 2008. *Proc. 7th International Topical Meeting on Nuclear Reactor Thermal Hydraulics, Operation and Safety (NUTHOS-7)* (CD-ROM), Paper 039.
7. Tanaka, M. et al. *U-RANS simulation of unsteady eddy motion in pipe elbow at high Reynolds number conditions*. 2010. *Proc. 2010 International Congress on Advances in Nuclear Power Plants (ICAPP '10)* (CD-ROM), pp. 1699-1708.
8. Eguchi, Y. et al. *Unsteady hydraulic characteristics in large-diameter pipings with elbow for JSFR, 2; Studies on applicability of a large-eddy simulation to high Re-number short-elbow pipe flow*. 2009. *Proc. 13th International Topical Meeting on Nuclear Reactor Thermal Hydraulics (NURETH-13)* (CD-ROM). N13P1162.
9. Ono, A. et al. *Influence of elbow curvature on flow structure at elbow outlet under high Reynolds number condition*. 2009. *Nuclear Engineering and Design*, doi: 10.1026/j.nuclearengdes.2010.09.026
10. Takamura, H. et al. *PIV measurement of a Complex Turbulent Flow in a Short Elbow Piping under a High Reynolds Number condition*. 2011. *Proc 9<sup>th</sup> International Symposium on Particle Image Velocimetry* (Flash Memory)
11. Ebara, S. et al. *PIV measurement for Dual Elbow Flow Using 1/7-Scale Model of Cold-Leg Piping in a Sodium-Cooled Fast Reactor*. 2010. *Proc. Seventh International Conference on Flow Dynamics (ICFD-7)*, pp. 108-109
12. Philip Holmes. et al. *Turbulence, Coherent Structures, Dynamical Systems and Symmetry*. 1998. Cambridge University Press.